ELSEVIER

Earth and Planetary Science Letters 121 (1994) 137–152

EPSL

Erosion processes in volcanic conduits and application to the AD 79 eruption of Vesuvius

Giovanni Macedonio [a], Flavio Dobran [b], Augusto Neri [c]

[a] *CNR-Centro di Studio per la Geologia Strutturale e Dinamica dell'Appennino, Via S. Maria 53, 56100 Pisa, Italy*
[b] *Department of Earth System Science, New York University, New York, N.Y. 10003, USA, and Istituto Nazionale di Geofisica, Rome, Italy*
[c] *GNV, Universita di Pisa, Via S. Maria 53, 56100 Pisa, Italy, and Istituto Nazionale di Geofisica, Rome, Italy*

(Received January 4, 1993; revision accepted October 2, 1993)

Abstract

The flow of gas, magma and pyroclasts through a volcanic conduit produces erosion of the conduit wall. Erosion may be produced by the impact of pyroclasts on the conduit wall, fluid shear stress at the wall, conduit wall collapse, and volcanic tremor. Using a two-phase flow non-equilibrium model of magma ascent along the volcanic conduits demonstrated that the erosion due to the impact of particles on the wall can occur only above the magma fragmentation level of the conduit where the particles or pyroclasts remove the wall material by an abrasion process. This abrasion process was found to be the largest near the conduit exit where the gas–magma velocities are the largest. The erosion due to the fluid shear stress at the wall can be produced along the entire length of a conduit, depending on the wall roughness and yield strength of wall rocks. This shear stress is the largest near the magma fragmentation level where the gas–magma viscosity and velocity gradients are very large. The collapse of conduit wall due to the difference between the gas–magma and lithostatic pressures can occur below and above the magma fragmentation level, causing the production of lithics directly when the wall collapses inward, and indirectly when the wall collapses outward. The effectiveness of different erosion mechanisms was tested with the magma characteristics, conduit geometry, and wall rock properties pertaining to the AD 79 eruption of Vesuvius. It was found that during the white and gray magma plinian eruption phases the lithics should had come from the deep as well as from the shallow regions of the conduit. The conclusions from erosion modeling are also consistent with the limited field data whereby the gray magma phase deposits are associated with larger lithic content and larger proportion of deep limestone fragments.

1. Introduction

During a volcanic eruption, the flow of magma, gas and pyroclasts through a conduit can produce erosion or abrasion of the conduit wall. The fluid flow can also produce pressures which are different from lithostatic in the magma chamber and along the conduit, causing the production of lithics due to wall collapses. The erosion depends, therefore, on the thermofluid-dynamic characteristics of the multiphase mixture of magma, crystals and gas flowing in the conduit as well as on the lithology of the volcanic edifice. A

[PT]

SSDI 0012-821X(93)E0216-7

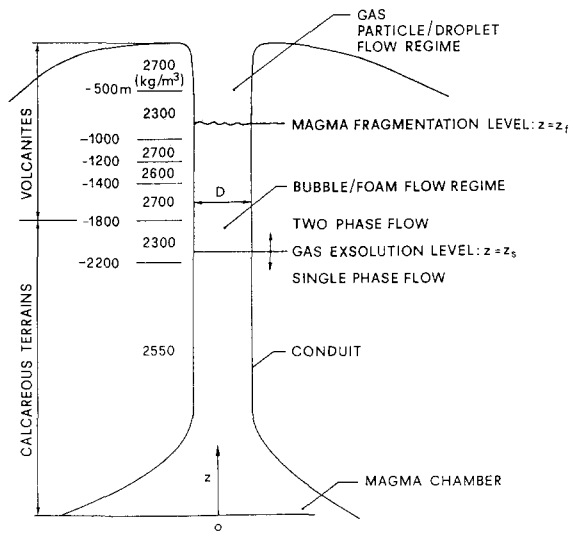

Fig. 1. Illustration showing a possible volcanic conduit of Vesuvius during the AD 79 plinian eruption. The magma is accelerated from stagnation state o in the magma chamber and begins exsolving at $z = z_s$ and fragmenting at $z = z_f$. The stratigraphy of the conduit wall is indicated by seven different zones with associated rock densities.

typical condition of the rising magma through a conduit or fissure is depicted in Fig. 1. The mixture of magma and crystals ascends from a magma chamber at $z = 0$ and the dissolved gases in the magma begin exsolving at $z = z_s$. For $z > z_s$, the exsolved gas forms bubbles which grow as the magma ascends toward the surface. The bubbly two-phase flow mixture subsequently fragments at $z = z_f$ where the bubble packing density in magma reaches a maximum. Above the magma fragmentation level, the two-phase flow regime consists of liquid magma drops or particles (pyroclasts) flowing in a continuous gas phase. The changing magma flow regimes along a conduit in combination with the changing stratigraphy of the conduit wall rocks can lead not only to different erosion rates or production of lithics along the conduit, but also to different mechanisms which can cause the erosion.

In the course of a volcanic eruption the ratio of lithics to juvenile products can vary. The lithics may come from the breakup of the walls of the magma chamber and conduit wall abrasion due to fluid flow [1], as well as from wall collapses due to the changing magma pressure in the conduit [2–4]. A magma–water interaction in a conduit can also cause erosion due to the change of pressure on the conduit wall [5] and propagation of shock and stress waves [6]. The eruptions of Vesuvius in AD 79 and 1906 [7–9] and the prehistoric eruption of Nisyros [8] provide evidence of different ways in which non-juvenile volcanic fragments can be intermixed with juvenile products during the course of an eruption.

Finnie [10,11] considered the erosion of ductile materials by a stream of solid particles. He developed a theory of two-dimensional erosive cutting and noted that the factors which may influence the ductile erosion include the particles' angle of impingement, rotation, velocity, size, shape, strength and concentration, and the properties and shape of the surface being eroded. This cutting theory predicts that the removed surface volume is proportional to the mass of the eroding particles, the square of the particle velocity and the angle of impact of the particles which produces a maximum erosion at about 20°, and inversely proportional to the surface hardness. Nielson and Gilchrist [12] performed experiments with particle laden gas streams and different material particles. They found that for glass the predominant erosion mechanism is due to the cracking of the surface by force components of particles which are normal to the erosion surface, whereas for ductile materials the cutting wear described by Finnie is also important. In applications to fluidized beds, Bouillard et al. [13] and Lyczkowski et al. [14] extended the power dissipation erosion model of Ushimaru et al. [15] and developed a monolayer energy dissipation (MED) erosion model where the second law of thermodynamics and kinetic and total energy equations of a mixture of gas and solid particles were used to establish the following rate of kinetic energy dissipation:

$$D_k = tr(\alpha\tau_G\nabla v_G) + tr((1-\alpha)\tau_S\nabla v_S) + (v_G - v_S)^2\beta \geq 0 \quad (1)$$

where α is the volumetric fraction of gas in the mixture, τ is the viscous stress tensor, v is the velocity, β is the gas–particle drag coefficient, tr denotes the mathematical operation of trace, and

the subscripts G and S pertain to the gas and solid particles respectively. The rate of kinetic energy dissipation given by Eq. (1) in a monolayer of particles in the vicinity of a stationary surface can be converted to: (a) heat which is produced between the gas and solid particles, between the gas and surface, and between the particles and surface; (b) erosion of the surface; (c) attrition of solid particles. The rate of kinetic energy dissipation which can result in erosion is clearly only a fraction of the total energy dissipation rate given by Eq. (1). The MED model accounts for the kinetic energy dissipation by one layer of particles in the proximity of an eroding surface which is then converted into an erosion rate.

The lateral blast of Mount St. Helens on May 18, 1980 produced erosional features or furrows on or near ridges which Kieffer and Sturtevant [16] attribute to the erosional nature of longitudinal vortices aligned with the flow direction. In order for such erosional features to occur it is necessary that a high-speed flow traverses complex topography, becomes unstable, and produces large-scale vortical motions in turbulent shear flow. It is difficult to visualize, however, how such an organized flow behavior may be operative in internal flow passages such as volcanic conduits where the fluid mechanic characteristics are very different from external flows.

Depending on the gas–magma flow regime in a volcanic conduit, it is possible to identify several basic erosion mechanisms. Erosion can be produced due to the impact of solid particles on the conduit wall whereby the particles cut, deform or crack the surface, leading subsequently to the stripping of the surface material. As such, this erosion mechanism is possible only above the magma fragmentation level where the gas viscosity does not impede greatly the motion of solid particles. Erosion can also be produced by the effect of the shear stress of the flowing fluid on the conduit wall. This type of erosion acts along the whole length of the conduit, both below and above the magma fragmentation level, and should be at its greatest where the viscosity and velocity gradients of the flowing mixture attain their largest values along a conduit. In establishing the total inflow of wall material into the conduit it is also necessary to consider the generation of lithics from the conduit wall collapses produced by the difference between the lithostatic and fluid pressures. Such a production mechanism for lithics may indeed be very important because it may contribute to the fracture of rocks along the whole conduit, and in particular near the magma fragmentation level where the magma pressure can fall considerably below the local lithostatic pressure [2–4]. Another possible wall erosion mechanism can be associated with the volcanic tremor which can be produced by a buoyantly rising magma which fractures the rocks, or by the fluid-dynamic phenomena in the conduit associated with bubbles and motion of exsolution, fragmentation and shock wave fronts during the changing magma flow conditions.

This paper has the following objectives: (1) to demonstrate how the non-equilibrium two-phase flow model of Dobran [2] and Papale and Dobran [3] describing magma transport in volcanic conduits can be used to determine the regions in conduits which are most susceptible to erosion, and (2) to test the model predictions with the lithics data for the white and gray magma eruption phases of Vesuvius in AD 79. It will be shown that in the neighborhood of the magma fragmentation level the fluid shear stress can be very large and can contribute significantly to the abrasion of the wall material, and that near this level the large difference between the lithostatic and fluid pressures can also produce a conduit wall collapse or an inflow of wall rocks or lithics into the conduit, whereas near the conduit exit the moderate increase of gas–magma pressure above the lithostatic pressure and large gas–magma velocities and velocity gradients may be responsible for significant conduit erosion or formation of a vent.

2. Magma flow and erosion modeling in conduits

2.1. Fluid dynamic modeling

Dobran [2] developed a steady-state, one-dimensional and two-phase flow non-equilibrium model for the gas–magma flow in volcanic con-

duits. In this model the ascending magma with crystals is assumed to flow as a single-phase fluid until it begins to exsolve the dissolved water at the height z_s above a magma chamber (Fig. 1). For $z > z_s$ and below the magma fragmentation, $z < z_f$, the exsolved gas in the form of bubbles forms a two-phase bubbly flow mixture, whereby the gas bubbles are contained in the continuous liquid magma with crystals. Above the magma fragmentation level, $z \geqslant z_f$, the two-phase flow regime consists of a continuous gas phase with dispersed drops or particles of fragmented magma.

The single-phase flow length z_s can be established on the basis of the exsolution pressure P_s by applying a one-dimensional form of the momentum equation between the stagnation state o in the magma chamber and the height z_s in the conduit [2,3,17]. In this paper the magma chamber pressure was computed on the basis of the density distribution or stratigraphy as indicated in Fig. 1. In the application of the magma flow model to Vesuvius as described below, the stratigraphy of the volcanic edifice of Vesuvius was divided into seven layers [3], and is based on the data of Balducci et al. [18] who drilled a deep exploration well (Trecase-I) about 2000 m from the Somma–Vesuvius caldera and about 2000 m deep. The upper layers, from 0 to 1800 m below the crater rim, are made of volcanic material and will be referred to in this paper as 'volcanites'. The lower layers are made of carbonatic conglomerates, limestones and dolomites, and will be referred as 'calcareous terrains' or the Italian, '*calcari*'. The stratigraphy of the wall rocks near the conduit of the AD 79 eruption of Vesuvius was probably somewhat different from that assumed above due to the subsidence of the central portion of the volcanic complex as the result of subsequent eruptions.

Above the gas exsolution level, $z \geqslant z_s$, the two-phase flow can be modeled by the equations expressing the conservation of mass and balance of momentum of gas and liquid [2]. Thus,

$$G_G = \rho_G \alpha u_G \tag{2}$$

$$\frac{dG_L}{dz} = \frac{d}{dz}\rho_L(1-\alpha)u_L = \hat{C}_w \tag{3}$$

$$\rho_G u_G \alpha \frac{du_G}{dz} = -\alpha \frac{dP}{dz} - F_{LG} - F_{wG} - \rho_G g \alpha \tag{4}$$

$$\rho_L u_L (1-\alpha)\frac{du_L}{dz} = -(1-\alpha)\frac{dP}{dz} + F_{LG} - F_{wL} + \hat{C}_w(u_w - u_L) - \rho_L g(1-\alpha) \tag{5}$$

where α is the gas volumetric fraction, u is the vertical velocity and $\hat{C}_w$ is the mass erosion rate per unit volume. The subscripts G and L refer to the gas and liquid phases, respectively, with L denoting the liquid magma and crystals below the magma fragmentation level and magma drops or solid particles above the magma fragmentation level. The velocity u_w is the velocity of the material being eroded and introduced into the flowing mixture in the conduit. The interphase and wall friction terms F_{LG}, F_{wG} and F_{wL} account for the gas–liquid drag, gas–wall drag and liquid–wall drag, respectively, and are specified by the appropriate constitutive equations depending on the flow regime [2]. The magma viscosity [19], gas exsolution [20] and density [21] depend on magma composition and were modeled according to the models described in Papale and Dobran [3,4].

The erosion modeling by the above steady-state model also requires the specification of the mass erosion rate $\hat{C}_w$, which will be assumed to be negligible in the modeling Eqs. (5)–(8), but will be estimated *a posteriori* to establish the relative importance of different erosion mechanisms in different regions of a volcanic conduit. This modeling approach is reasonable as long as we are only interested in identifying the importance of different erosion mechanisms and not in quantifying these mechanisms in detail. Once an erosion is initiated, the results from the above model must be carefully evaluated, since they are not expected to be valid when the erosion rate is large or the erosion mass and momentum fluxes contribute significantly to the gas and magma fluxes along the conduit.

2.2. Erosion due to impact of particles on the conduit wall

Erosion due to the impact of particles on the conduit wall is possible only above the magma

fragmentation level. This level is defined by the gas volumetric fraction $\alpha = 0.75$ which corresponds to the maximum packing density of the bubbles [2,22]. The erosion rate is assumed to be proportional to the power dissipated by interparticle collisions in a layer ('monolayer') of particles near the wall surface. The rate of kinetic energy dissipation D_k due to the interparticle drag is then given by

$$D_k = \beta(\boldsymbol{v}_G - \boldsymbol{v}_S)^2 \tag{6}$$

where β is the gas–particle drag coefficient which is related to the gas–particle drag according to $F_{LG} = \beta|\boldsymbol{v}_G - \boldsymbol{v}_S|$. The dissipated power of particles near the wall may be obtained by assuming that $\boldsymbol{v}_G \approx 0$ near the wall and that the particles inelastically collide with the wall with a restitution coefficient e. The power dissipation per unit volume δD_k due to the particle collisions with the wall is then given by

$$\delta D_k = \beta \delta u_S^2 = \beta(1+e^2)u_S^2 \tag{7}$$

The dissipated power in a monolayer of volume V can be related to the thickness of the layer b and the wall surface area S, where $V = bS$. Integrating Eq. (7) over the volume V produces the dissipation power $\dot{P}_e$ which can be expressed as follows:

$$\dot{P}_e = \int_V \delta D_k \, dV = \beta(1-e^2)u_S^2 bS \tag{8}$$

The dissipated power which is needed to remove the material from a conduit wall may thus be expressed by the following equation:

$$\dot{P}_e = \tau_B S \dot{E} \tag{9}$$

where τ_B is the yield stress of the wall rocks and $\dot{E}$ is the erosion rate (m/s). Combining Eqs. (8) and (9) and noting the relationship between $\dot{E}$ and $\hat{C}_w$ produces the erosion rate from particle collisions with the wall:

$$\dot{E} = \frac{(1-e^2)}{\tau_B}\beta u_s^2 b = \frac{\hat{C}_w}{\rho_w}R_c \tag{10}$$

where R_c is the ratio between the conduit cross-sectional area and the conduit perimeter ($D/4$ for circular conduits). It should be noted in the above erosion rate formula that the effect of particle hardness can be accounted for by the restitution coefficient e. Since above the magma fragmentation surface the magma conditions can change from liquid to solid pyroclasts, it is clear that e is a local function of this change and needs to be modeled appropriately.

2.3. Erosion due to fluid shear stress at the wall

The model of the erosion due to the fluid shear stress at the wall assumes that the erosion is due to the fluid viscosity. By considering a fluid flowing in a conduit with a rough surface and roughness height l_r it can easily be seen that the forces which act on this roughness height are due to the fluid shear stress τ_w near the wall, the pressure gradient dP/dz, and gravity. The erosion of the wall rock or breakage of the wall surface roughness may then be possible when the sum of these forces exceeds the yield strength of the rocks τ_B, i.e.

$$\left|\tau_w - \frac{dP}{dz}l_r - \rho_w g l_r\right| \geq \tau_B \tag{11}$$

The erosion rate due to the wall shear stress is then assumed to be proportional to the power dissipated by the fluid near the surface in a layer with a thickness equal to the roughness height of the wall l_r and volume $V = Sl_r$. Thus,

$$\dot{P}_e = \int_V C_1 tr(\boldsymbol{\tau}\nabla\boldsymbol{v}) \, dV = C\left|\frac{\partial u}{\partial y}\right|_w^2 \mu_m l_r S \tag{12}$$

where μ_m is the two-phase flow mixture viscosity [2] and y is the coordinate perpendicular to the wall surface. The constants C_1 and C are empirical parameters which should be determined from the experimental data by comparing the integrated values of erosion rates along a conduit with field data. Using Eqs. (9) and (12) the erosion rate by the fluid shear stress at the wall becomes

$$\dot{E} = C\left|\frac{\partial u}{\partial y}\right|_w^2 \frac{\mu_m l_r}{\tau_B} = \frac{\hat{C}_w}{\rho_w}R_c \tag{13}$$

2.4. Erosion due to conduit wall collapse

A gas–magma flow in a volcanic conduit can produce a pressure which can be smaller or larger

than the local lithostatic pressure [2–4]. This pressure difference can produce a fracture of the conduit wall when the stress failure criterion of rocks is exceeded. By assuming that the rocks behave elastically, the criterion for failure of rocks can be estimated from the following expression [5]:

$$| P - P_{\text{lith}} | \geq 2\tau_{\text{T}} \tag{14}$$

where τ_{T} is the minimum or tensile strength of rocks, which ranges from 0.1 (for highly fractured and sedimentary rocks) to 10 MPa (for pristine basalt and granite) [23]. It should be noted that the wall collapse criterion expressed by Eq. (14) accounts for the inward and outward wall collapses. In the former case the lithics are introduced directly into the conduit, whereas in the latter indirect case an additional mechanism such as the shear stress produced by the fluid friction is required for the broken wall material to be entrained or removed from the wall region. The eroded mass due to these collapses is not easy to quantify without introducing many other poorly constrained parameters but it should depend on the overpressure and underpressure of the rocks with respect to the lithostatic pressure, stress states of local rocks, and on the lithology of the volcanic edifice which surrounds the magma chamber or conduit.

2.5. Erosion due to volcanic tremor

The sustained low-frequency (0–10 Hz) ground motions lasting a few minutes to several days and associated with volcanic events are termed the volcanic tremors [24–26]. The origin of these low-frequency volcanic earthquakes appears to be associated principally with the pressure oscillations in the ascending magma, either propagating through the cracks or through a volcanic conduit. These pressure oscillations can cause the displacement of the fluid-filled fractures or conduit wall and generate elastic waves in the surrounding rock. The pressure oscillations in an erupting magma can be associated with the changing magma composition at depth which can subsequently produce changes in the exsolution and fragmentation levels in a conduit [3,4]. This can in turn produce changes in the differences between the lithostatic and fluid pressures, leading to the conduit-wall oscillations and possibly fracturing. The erosion due to the volcanic tremors is thus difficult to quantify and can both cause and be affected by the erosion mass flux.

2.6. Total erosion rate

The total mass eroded due to the impact of particles on the conduit wall and due to the fluid shear stress at the wall is obtained by combining the results expressed by Eqs. (10) and (13):

$$\hat{C}_{\text{w}} = \frac{\rho_{\text{w}}}{\tau_{\text{B}} R_{\text{c}}} \left((1 - e^2) \beta u_{\text{S}}^2 b + C \left| \frac{\partial u}{\partial y} \right|_{\text{w}}^2 \mu_{\text{m}} l_{\text{r}} \right) \tag{15}$$

It should be noted, however, that the two erosion processes consisting in the impact of particles with the wall and fluid shear stress at the wall should not be considered independently of each other; rather it is useful to consider these mechanismsas as the basic erosion mechanisms. As noted above, the eroded mass due to the wall collapse and volcanic tremor are not easy to quantify, but should be added to the production of lithics in Eq. (15) for an estimate of the total erosion rate in a volcanic conduit.

2.7. Stratigraphy of the deposit and input data for modeling

The two-phase flow model described in Section 2.1 requires input information in the form of magma composition and crystal content, temperature and pressure in the magma chamber, conduit geometry, and stratigraphy and physical data on the conduit wall rocks [2,27]. For an application of this model to the AD 79 eruption of Vesuvius the stratigraphy of the rocks surrounding the conduit wall was obtained from the data of Balducci et al. [18], as shown in Fig. 1, and on this basis the magma chamber pressure was established according to Eq. (4). Although the model assumes steady-state conditions of magma in magma chamber and conduit, it should be noted that the erosion processes are transient and may lead to changes in the conduit geometry which

can be reflected in the variation of the mass eruption rate during an eruption [28] [1]. The withdrawal of magma from a magma chamber causes the pressure in the chamber to decrease, which may be estimated in the manner proposed by Druitt and Sparks [29] if the magma chamber parameters can be estimated. For Vesuvius, such an estimate would be very speculative [30]. A magma chamber pressure decrease during eruption will produce lower pressures in the conduit which will have a tendency of further promoting inward wall collapses.

During the AD 79 plinian eruption of Vesuvius a volume of about 3 km^3 of ash and pumice was erupted in a very short time (in less than 30 hours) [31], with a maximum eruption rate exceeding 10^8 kg/s [32,33]. The beginning of the eruption is marked by a thin layer of coarse ash with *calcari* and lava fragments [34] which is covered by a thick fallout layer consisting of pumice of phonolitic composition in its lower portion (white pumice) and of tephritic–phonolitic composition in the upper portion (gray pumice). The sequence continues with intermixed layers from surges and pyroclastic flows, and fine ash. During the entire eruptive sequence, the nature of the lithics remained essentially unchanged. The lithic/juveniles ratio in the deposit depends on the distance from the vent, but the existing data are of limited usefulness in identifying the provenance of the lithics from within the conduit.

Lirer et al. [31] studied about 30 scattered sections of the pumice fall deposit of the AD 79 Vesuvius eruption and found minor, but constant, variations in the content of lithic fragments within the succession. They show the lithic content to be 12 wt% for the white, and 20 wt% for the gray deposit, with an increase in the proportion of limestone fragments (*calcari*) from the lower to the upper layer. Sheridan et al. [32] confirmed the occurrence of an increase in the lithic content and in the proportion of limestones from the white to the gray pumice layer. Barberi et al. [34] performed detailed granulometric and component distribution analyses on two different sections of the AD 79 sequence which are located at 3.5 and 14 km from the vent along the main dispersal axis. Table 1 illustrates a decrease in the lithics content for the more proximal section and an increase in the content of lithics and proportion of carbonate fragments for the distal section when passing from the white to the gray pumice deposit. Cioni et al. [35] found that at least in the proximal southeastern part of the area of deposition the limestones or *calcari* are more abundant in the gray than in the white pumice fall deposit, whereas an increase in the lithics content is detectable in the central (more than 6 km from the present crater) southeastern part. Much of the data for the AD 79 fallout deposit are consistent with an increase in lithics and of the proportion of calcareous rocks from the white to the gray deposit.

Table 1
The white and gray pumice lithics ratios [34]

Position	White pumice		Gray pumice	
	lithics/ juv.	*calcari* / volcanites	lithics/ juv.	*calcari* / volcanites
3.5 km from the vent	0.72	0.24–0.26	0.46	–
14 km from the vent	0.28	0.42–0.52	0.53	0.63

The maximum discharge rates of the white (8×10^7 kg/s) and gray (1.5×10^8 kg/s) magmas as obtained by Carey and Sigurdsson [36] were modeled by assuming that these flow rates are the maximum possible discharges through the conduit, which corresponds to the choked-flow condition at the conduit exit. The depth of the magma chamber of Vesuvius in AD 79 is constrained between 3 and 5 km [37], and for the purpose of this paper was assumed to be located at 5 km. The magma temperature was assumed to be 1073 K for the white and 1120 K for the gray magma [1,3]. The white magma density and dissolved water content were taken as $\rho_L = 2400$

[1] The steady-state flow assumption for the simulation of the magma ascent during the AD 79 Vesuvius and May 18, 1980 Mt. St. Helens eruption phases without taking into account the erosion processes have been discussed by Papale and Dobran [3,4].

kg/m^3 and $Y = 4.7$ wt% respectively, whereas the density and water content of gray magma were taken as $\rho_L = 2550$ kg/m^3 and $Y = 3.5$ wt% [2,3,38]. These and other data pertaining to the white and gray magmas, physical properties of the rocks, and estimates of the parameters for erosion modeling are summarized in Table 2 where the magma chamber pressure P_0 corresponds to the lithostatic load. Using the data from Table 2 and the physical model of magma flow described above allowed the determination of erosion rates in different parts of the conduit.

3. Results

Figs. 2–5 illustrate the distributions of pressure, gas volumetric fraction, and erosion rates along the conduit for the white and gray magma compositions of the AD 79 eruption of Vesuvius based on the magma chamber pressure given in Table 2. The corresponding conditions for erosion by the fluid shear stress at the wall and due to the conduit wall collapse are shown in Figs. 6–9.

The white and gray magma pressure distributions along the conduit illustrated in Figs. 2 and 3 show that the pressure of gas and magma in the conduit can be above or below the lithostatic pressure. Below the magma fragmentation zone,

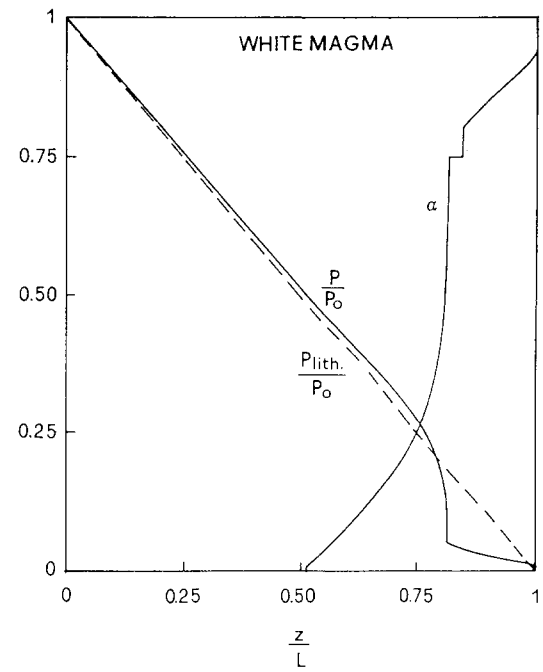

Fig. 2. Gas volumetric fraction and gas–magma and lithostatic pressure distributions along the conduit for the white magma eruption phase of Vesuvius in AD 79.

the white magma produces pressures above the lithostatic, whereas the gray magma produces pressures below the lithostatic. As the water is exsolved from magma causing an increase in its

Table 2
Input data for the magma and erosion models pertaining to the AD 79 eruption of Vesuvius

	White magma	Gray magma
Conduit length L (m)	5000	5000
Mass eruption rate $\dot{m}$ (kg/s)	8×10^7	1.5×10^8
Magma temperature T (K)	1073	1120
Dissolved water content Y (wt%)	4.7	3.5
Magma chamber pressure P_0 (MPa)	127 (lithostatic)	127 (lithostatic)
Magma density ρ_L (kg/m^3)	2400	2550
Volumetric crystal fraction ϕ_L	0.241	0.234
Fragmented particle diameter d_L (μm)	200	200
Restitution coefficient e	0.5	0.5
Wall roughness height l_r (m)	1	1
Monolayer thickness b (m)	1	1
Dissipation constant C	1	1
Conduit wall yield stress τ_B (MPa)	0.2, 2, 10	0.2, 2, 10
Tensile strength of rocks τ_T (MPa)	0.1, 1, 5	0.1, 1, 5
Wall density ρ_w (kg/m^3)	from stratigraphy	from stratigraphy

viscosity due to the increasing strength of the covalent SiOSi bonds [39], and, as the gas bubbles increase in size mainly due to decompression and their motion relative to the magma is prevented by the high magma viscosity, the large frictional pressure drop causes a rapid fluid pressure decrease below the local lithostatic pressure near the magma fragmentation level. For the white magma composition this fluid pressure decrease below the lithostatic pressure is about 16 MPa (Fig. 2), which contrasts with about 8 MPa (Fig. 3) for the gray magma composition. After the magma fragments, the rate of magma pressure decrease becomes less steep than that of the lithostatic pressure, and the mixture of gas and particles exits from the vent at a pressure above the atmospheric pressure. The white magma also has deeper exsolution and fragmentation levels than the gray magma. The choked flow conditions of the white and gray magmas at the conduit exit require conduit diameters of 84 and 91 m, respectively, which are consistent with previous modeling of the AD 79 plinian eruption of Vesuvius [2,3].

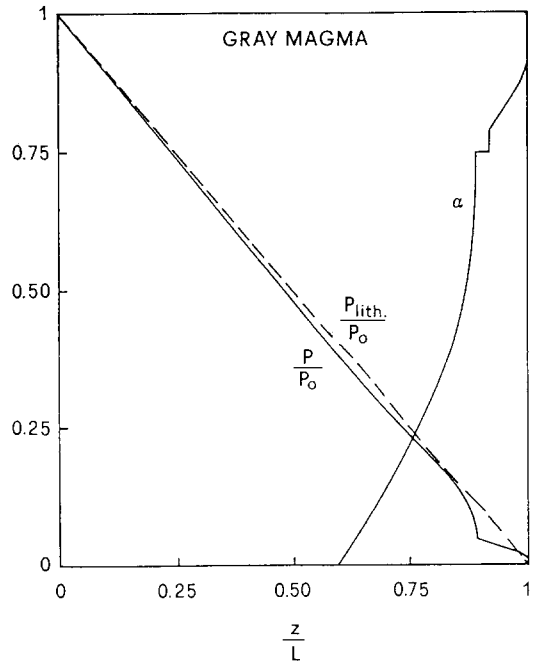

Fig. 3. Gas volumetric fraction and gas–magma and lithostatic pressure distributions along the conduit for the gray magma eruption phase of Vesuvius in AD 79.

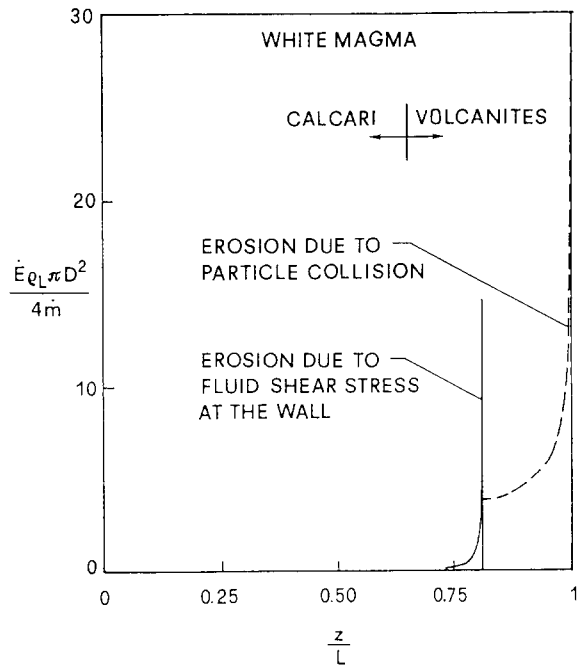

Fig. 4. Non-dimensional distributions of erosion rates along the conduit due to fluid shear stress at the wall below the magma fragmentation level and due to impact of particles with the wall above the magma fragmentation level for the white magma eruption phase.

The erosion rates computed from Eqs. (14) and (17) and non-dimensionalized with respect to the magma flow velocity ($4\dot{m}/\rho_L\pi D2$) are plotted in Figs. 4 and 5 for the white and gray magma compositions, respectively. The white magma (Fig. 4) produces more significant erosion due to the fluid shear stress at the wall below the magma fragmentation level (located at $z/L \approx 0.8$) than the gray magma (Fig. 5), which has this level located at $z/L \approx 0.9$. Above the magma fragmentation level, the erosion due to the fluid shear stress at the wall is greatly reduced because of the enormous decrease in the fluid viscosity. The erosion due to the impact of particles above the magma fragmentation level increases for both magmas toward the conduit exit where the flow is choked and the erosion rate increases considerably due to the large gas and pyroclasts velocities

and velocity gradients in this region. This implies that the exit region of the conduit should be subject to the formation of a vent, which is consistent with almost every explosive eruption [28].

For erosion due to fluid shear stress at the wall of a volcanic conduit to occur it is necessary that the erosion rate satisfies the *condition for erosion* as given by Eq. (11). Figs. 6 and 7 illustrate this situation for the white and gray magmas when the rock yield stresses are assumed to be equal to 0.2, 2, and 10 MPa. The gray magma, with its associated lower erosion rate due to the fluid shear stress at the wall, does not produce wall erosion with rock yield stresses which are larger than about 3 MPa, even near the magma fragmentation level. For both the gray and white magmas, the erosion due to the fluid shear stress at the wall is localized and may thus become significant only near the magma fragmentation level.

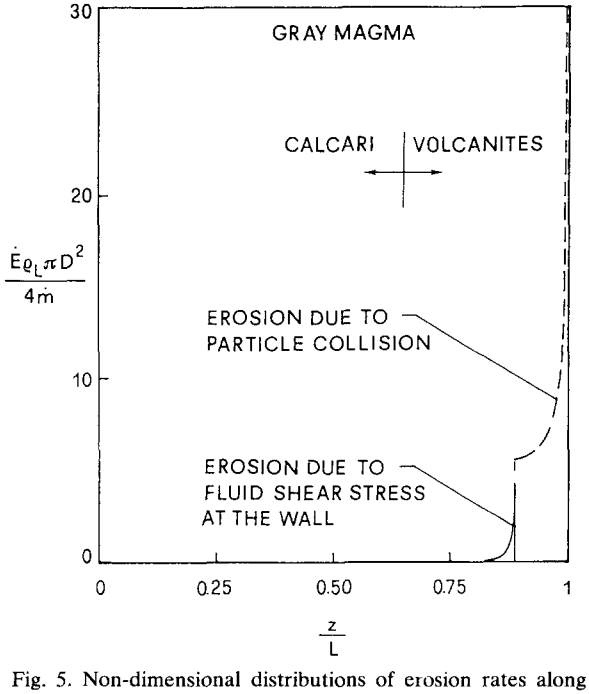

Fig. 5. Non-dimensional distributions of erosion rates along the conduit due to fluid shear stress at the wall below the magma fragmentation level and due to impact of particles with the wall above the magma fragmentation level for the gray magma eruption phase.

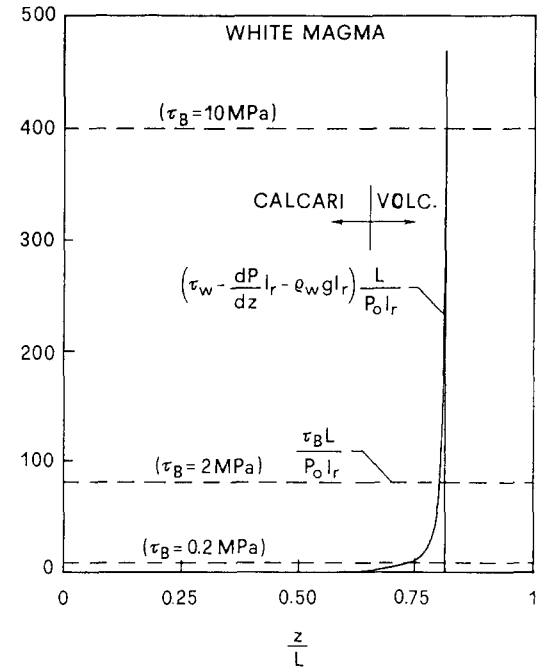

Fig. 6. Conditions for erosion due to the fluid shear stress at the wall for the white magma as a function of the rock yield strength.

The non-dimensional distribution of the absolute difference between the fluid and lithostatic pressures along the conduit is illustrated in Fig. 8 for the white magma and in Fig. 9 for the gray magma. The regions with SW–NE shading indicate where the fluid pressure is above the lithostatic pressure, whereas the regions with SE–NW shading represent the situation where the fluid pressure is below the lithostatic pressure. In these figures the conditions for erosion due to conduit wall collapse, as expressed by the tensile strength of the rocks or the condition given by Eq. (14), are also shown. For low values of τ_T, both the *calcari* and the volcanites are subject to wall collapses over significant lengths of the conduit for both magma types. For the white magma, the wall collapse should be outward, whereas for the gray magma the collapse should be inward, for almost the entire length of the conduit below the magma fragmentation level. Above the magma fragmentation level, the wall collapse should be inward for both magma types, except near the

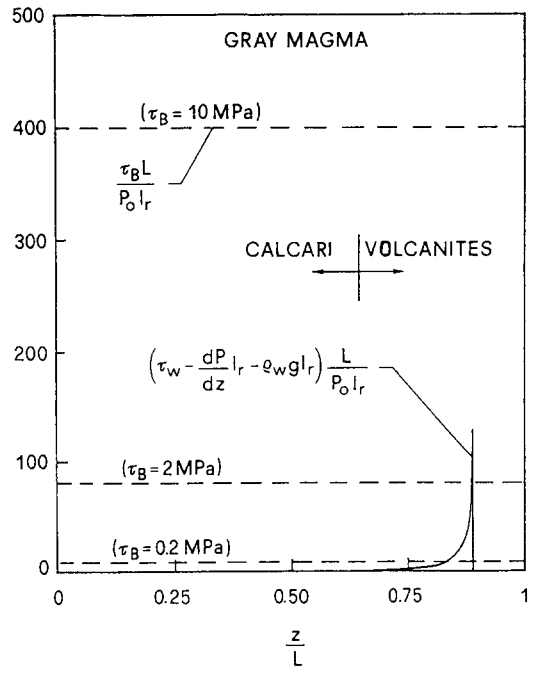

Fig. 7. Conditions for erosion due to the fluid shear stress at the wall for the gray magma as a function of the rock yield strength.

conduit exit where the gas magma pressure is above the lithostatic pressure; outward wall collapse may occur here. The variations in the ratio between the lengths of the regions associated with the eroded calcareous material in the lower part of the conduit and with the volcanites eroded in the upper part of the conduit are significant and may be used to compare qualitatively the results from the erosion modeling with the field data on white and gray pumices in Table 1.

4. Discussion

The white magma of the AD 79 eruption of Vesuvius shows a larger absolute difference between the gas–magma and lithostatic pressures near and above the magma fragmentation level, and a larger fluid pressure gradient in the neighborhood of this level than the gray magma (Figs. 2 and 3). These effects can in turn produce large erosion by the mechanisms fluid shear stress at the wall (Figs. 4 and 5) and wall collapse (Figs. 8 and 9). The erosion rate due to the fluid shear stress at the wall becomes significant in the vicinity of the magma fragmentation level and may produce a large erosive mass flux if the rocks are poorly consolidated in this region. In particular, the erosion rate produced by the white magma is greater than that produced by the gray magma. The rock yield stress criterion of 0.2 MPa, assumed to produce the erosion as shown in Figs. 6 and 7, represents, therefore, the fractured rock types [22] which may be easily produced by large differences between the fluid and lithostatic pressures created by the flowing magma. In this way, the production of lithics below the magma fragmentation level during the white magma eruption phase is governed principally by the conditions of the outward wall collapse, whereas their transport through the conduit occurs by the fluid shear stress at the wall. For the gray magma, however,

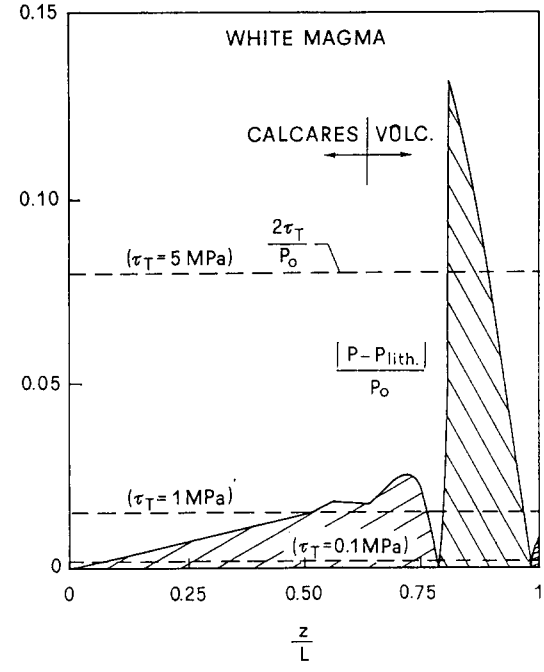

Fig. 8. Conditions for erosion due to the conduit wall collapse for white magma as a function of the tensile strength of the wall rocks. The regions with SW–NE shading indicate that the gas–magma pressure is above the lithostatic pressure, whereas the regions with SE–NW shading represent the situation where the fluid pressure is below the lithostatic pressure.

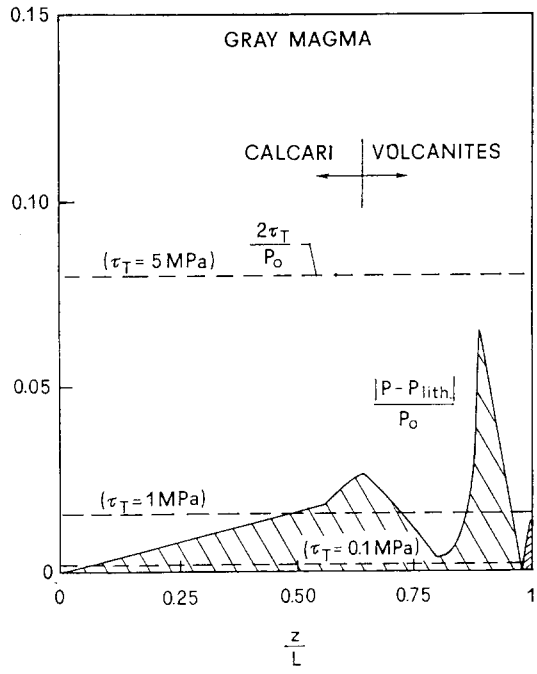

Fig. 9. Conditions for erosion due to conduit wall collapse for gray magma as a function of the tensile strength of the wall rocks. For explanation of the shaded regions, see Fig. 8.

the fluid pressure below the lithostatic pressure may produce inward wall collapses and favor a more efficient generation of lithics in the conduit. Above the magma fragmentation level, the lithics can be incorporated into the conduit by the conditions of the inward wall collapse and by the impacts of pyroclasts with the wall for both magmas, with a greater efficiency for the white magma. As shown in Figs. 8 and 9, the lithics from wall collapse can thus be produced from both the deep and the shallow regions of the conduit. Once rocks have been fractured by an outward wall collapse, or by an overpressure of flow with respect to the lithostatic pressure, they can be more easily removed by the frictional forces produced by the ascending magma. The large ratios of *calcari* to volcanites erupted during the gray magma eruption phase (see Table 1) reflect the modeling predictions and attest to the possibility of inward and outward wall collapses in producing the lithics during the AD 79 eruption of Vesuvius. The precise quantification of the rate of production of lithics by the wall collapse is not easy to estimate and should depend on the changing magma conditions at depth which can cause volcanic tremor and rock fracturing, and on the lithology of the volcanic rocks which surround the conduit, etc.

Near the conduit exit, the gas–pyroclast pressure exceeds the lithostatic pressure (Figs. 2 and 3) and the gas and pyroclasts attain large velocities and velocity gradients [2] which may cause large erosion rates due to the impact of particles on the conduit wall (Figs. 4 and 5). These large erosion rates should then easily form a crater near the surface where the rocks are generally poorly consolidated. Vent forming is a common feature in almost every explosive eruption and can thus be explained by the above erosion mechanisms. For a uniform diameter conduit as assumed in the magma flow model of Section 2.1, the choked flow condition is attained at the conduit exit, which must be therefore located at the base of the crater where the rocks are sufficiently consolidated to sustain large pressure and velocity gradients.

The precise estimation of the production of lithics due to the fluid shear stress at the wall, wall collapse and impact of particles on the conduit wall depends on several physical parameters which in general may be difficult to quantify. The erosion model due to the fluid shear stress at the wall requires the specification of wall roughness heigth l_r and of the dissipation constant C (Eqs. (11) and (13)). In the application of this model to Vesuvius use was made of $l_r = 1$ m (Table 2). A decrease of this height to below 1 m produces a lower erosion rate which should be more consistent with reality during the course of an eruption rather than during the initial stages of the eruption when the magma must channel its way toward the surface. A more reasonable value for this parameter may be of the order of 1 cm (or corresponding to the mean size of pyroclasts in the conduit), and this should produce more reasonable values for erosion rates than those shown in Figs. 4 and 5. The roughness height linearly increases the erosion rate (Eq. (13)), but unlike the monolayer thickness b (Eq. (10)), it determines the condition for erosion (Eq. (11)). Simi-

larly, the restitution coefficient e in the erosion model for impact of particles on the conduit wall (Eq. (10)) may vary from 0 to 1, depending on the state of the magma after fragmentation and on the fluid-dynamic processes and lithology of the wall rocks above the magma fragmentation level. A restitution coefficient equal to 0 corresponds to the transfer of particles to the wall and may occur in a region immediately above the magma fragmentation level where the magma has not cooled sufficiently. Under this condition the presented model of erosion due to particle collisions with the wall must break down, since this would correspond to the wall-forming process rather to the wall-erosion process. The monolayer thickness b linearly increases the erosion rate due to the particle collisions, and the assumed value of 1 m is probably too large, considering the generally small size of pyroclasts after the magma fragments and the small size of the lithics found in the deposits. The value of the dissipation constant $C = 1$ also overestimates the erosion rates reported in Figs. 4 and 5, since only part of the fluid's dissipative energy can be transformed into erosive wear. The value of this parameter may be determined by comparing the integrated values of erosion rates along a conduit with the erosion field data, if such data were available. For both the white and gray magma neither erosion rate parameters l_r, e and b, nor the wall stratigraphy, affect the ratios of the erosion rates pertaining to the erosion mechanisms fluid shear stress at the wall, impact of particles with the wall and wall collapse.

Data from Lirer et al. [31] coupled with the mass discharge rates from Carey and Sigurdsson [33] of 8×10^7 kg/s (white) and 1.5×10^8 kg/s (gray) for the plinian eruption phases of Vesuvius in AD 79 suggest peak erosion rates corresponding to a conduit diameter increase of about 20 m/h for the white and gray phases. This diameter increase is too large if account is taken of the duration of the eruption (about 18 h) and of the eruption dynamics during this time [3], implying that the data of Lirer et al. [31] are largely overestimates. However, the large conduit diameter increase suggests that the erosion processes along the conduit should not be equally effective along its entire length, but, according to the results of the present modeling, should be concentrated in particular regions of the conduit. Furthermore, it is probable that the conduit erosion and the transport of eroded fragments within the ascending magma are more effective during moments of the eruption which could correspond to changes in the flow dynamics, such as when the composition of the erupted magma changes from white to gray and the magmatic pressure drops from values larger than lithostatic to lower than lithostatic in deep regions of the conduit (Figs. 2 and 3). This can favor a more effective inflow of lithics from the conduit wall into the conduit in these deep regions and account for the larger proportion of limestone fragments in the deposit of the gray magma phase (which is also suggested by the wall collapse mechanisms) (Figs. 8 and 9). In addition, the decrease in magma chamber pressure due to magma withdrawal will also produce further pressure decrease below lithostatic in all regions of the conduit and thus favor more effective inward wall collapse events during the later stages of the eruption. A magma chamber pressure decrease of 10 MPa below the lithostatic rock load reported in Table 2 produces a drop of about 300 m in the magma fragmentation level during the gray eruption phase. As the magma changes from white to gray and magma chamber pressure decreases due to magma withdrawal, the magma fragmentation level is thus not expected to change significantly as reported in Figs. 2 and 3 and one should expect the lithics from deep conduit regions to be coated with magma and incorporated into pumice fragments. The extent of these effects at Vesuvius is not known at present. The testing of the present erosion mechanisms with data from other volcanoes is clearly problematic because this requires not only the availability of lithics data from deposits but also a knowledge of the eruption parameters which enter into the magma ascent model.

The erosion results obtained by the magma flow model described in Section 2.1 should be interpreted with caution due to the steady-state modeling in which the mass of the eroded material was ignored ($\hat{C}_w = 0$ in Eqs. (3) and (5)). The latter assumption is reasonable as long as the

erosion results are used only to interpret the relative importance of different erosion mechanisms and not to quantify these mechanisms.

5. Summary and conclusions

Using a non-homogeneous two-phase flow model of gas–magma flow along volcanic conduits allowed identification of the importance of several erosion mechanisms in the volcanic conduit of Vesuvius during the AD 79 white and gray magma plinian eruption phases. The erosion due to the impact of particles on the conduit wall was found to occur above the magma fragmentation level and to be important near the conduit exit where the velocities of gas and pyroclasts are the greatest in a constant diameter conduit. The erosion due to the fluid shear stress at the wall may become important only in a narrow region near the magma fragmentation level where the viscosity and velocity gradients become very large. The erosion due to the conduit wall collapse can become important below and above the magma fragmentation level of the conduit. When the gas–magma pressure is above the local lithostatic pressure, the outward wall collapse may fracture the rocks whereby the high wall shear stress of the flowing magma can subsequently remove the fractured wall fragments and transport them within the flow. When the fluid pressure falls below the lithostatic pressure, an inward wall collapse may produce directly an inflow of lithics into the conduit. This generation mechanism for lithics was found to be consistent with the abundant existence of *calcari* and volcanites in the deposits of the AD 79 eruption of Vesuvius, and with an increase in the ratio of *calcari* to volcanites during the change of eruption from white to gray magma eruption phases. However, the erosion data from the AD 79 eruption of Vesuvius are not of sufficient quality to allow the quantification of the different erosion mechanisms. A more complete modeling of erosion in volcanic conduits should be tied to the source of the magma at depth, to the lithology of the volcanic edifice, and to the transient fluid dynamic processes of the ascending magma. A much more comprehensive study of the origin of lithics within the conduit and their relationship with the eruption dynamics is badly needed for future progress in quantifying erosion processes. A more challenging task is to associate the identified erosion processes with the morphology of the lithic pyroclasts.

Nomenclature

b	monolayer thickness
$\hat{C}_w$	mass erosion rate per unit volume
C,C_1	constants in Eq. (12)
d	particle diameter
D	conduit diameter
D_k	kinetic energy dissipation
e	restitution coefficient
$\dot{E}$	erosion rate
F	drag force
g	gravitational constant
G	mass flow-rate per unit area
l_r	surface roughness height
L	conduit length
$\dot{m}$	ash flow-rate
P	pressure
$\dot{P}_e$	dissipation power
R_c	ratio of conduit cross-sectionional area/ perimeter
S	wall surface-area
u	vertical component of velocity
v	velocity vector
y	distance along normal to the conduit wall
z	distance along the conduit

Greek

α	gas volumetric or void fraction
β	gas–particle drag coefficient
μ	viscosity
ρ	density
τ	shear stress
τ_B	yield stress of wall rocks
τ_T	tensile strength of wall rocks
τ	stress tensor
ϕ	crystal fraction

Subscripts

f	fragmentation
G	gas
lith	lithostatic
L	magma and crystals or particles
m	mean or two-phase

o magma chamber
s exsolution
S solids or particles
w wall

6. References

[1] F. Barberi, H. Bizouard, R. Clocchiatti, N. Metrich, R. Santacroce and A. Sbrana, The Somma–Vesuvius magma chamber: a petrological and volcanological approach, Bull. Volcanol. 44, 295315, 1981.

[2] F. Dobran, Nonequilibrium flow in volcanic conduits and application to the eruptions of Mt. St. Helens on May 18, 1980, and Vesuvius in AD 79, J. Volcanol. Geotherm. Res. 49, 285–311, 1992.

[3] P. Papale and F. Dobran, Modeling of the ascent of magma during the plinian eruption of Vesuvius in AD 79, J. Volcanol. Geotherm. Res., in press., 1993.

[4] P. Papale and F. Dobran, Magma flow along the volcanic conduit during the plinian and pyroclastic flow phases of the May 18, 1980 Mt. St. Helens eruption, J. Geophys. Res., in press, 1993.

[5] F. Dobran and P. Papale, Magma–water interaction in closed systems and application to lava tunnels and volcanic conduits, J. Geophys. Res. 98, 14041–14058, 1993.

[6] F. Dobran, F. Barberi and C. Casarosa, Modeling of Volcanological Processes and Simulation of Volcanic Eruptions, Giardini, Pisa, 1990.

[7] V. Arnó, C. Principe, M. Rosi, R. Santacroce and A. Sbrana, Eruptive History, in: Somma–Vesuvius, R. Santacroce, ed.,. Quad. Ric. Sci.-CNR Roma 114(8), 53–103, 1987.

[8] F. Barberi, J.M. Navarro, M. Rosi, R. Santacroce and A. Sbrana, Explosive interaction of magma with ground water: insight from xenoliths and geothermal drillings, Rend. Soc. Ital. Mineral. Petrol. 43, 901–926, 1988.

[9] A. Bertagnini, P. Landi, R. Santacroce and A. Sbrana, The 1906 eruption of Vesuvius: from magmatic to phreatomagmatic activity through the flashing of a shallow depth hydrothermal system, Bull. Volcanol. 53, 517–532, 1991.

[10] I. Finnie, Erosion surfaces by solid particles, Wear 3, 87–103, 1960.

[11] I. Finnie, Some observations on the erosion of ductile metals, Wear 19, 81–90, 1972.

[12] J.H. Nielson and A. Gilchrist, Erosion by a stream of solid particles, Wear 11, 111–143, 1968.

[13] J.X. Bouillard, R.W. Lyczkowski, S. Folga, D. Gidaspow and G.F. Berry, Hydrodynamics of erosion of heat exchanger tubes in fluidized bed combustors, Can. J. Chem. Eng. 67, 218–229, 1989.

[14] R.W. Lyczkowski, J.X. Bouillard, G.F. Berry and D. Gidaspow, Erosion calculations in a two-dimensional fluidized bed, in: Proc. 9th Conf. Fluidized Bed Combustion, Vol. 2, pp. 697–706, ASME, New York, 1987.

[15] K. Ushimaru, C.T. Crowe and S. Bernstein, Design and application of the novel slurry jet pump, Energy Int. Inc. Rep. E184–108, 1984.

[16] S.W. Kieffer and B. Sturtevant, Erosional furrows during the lateral blast of Mount St. Helens, May 18, 1980, J. Geophys. Res. 93, 14793–14816, 1988.

[17] F.M. White, Fluid Mechanics, McGraw Hill, New York, 1979.

[18] S. Balducci, M. Vaselli and G. Verdiani, Exploration well in the Ottaviano permit, Italy: Trecase 1, in: Proc. 3th Int. Semin. Results of the EC Geothermal Energy Research (Munich), pp. 407–418, Reidel, Dordrecht, 1985.

[19] H.R. Shaw, Viscosities of magmatic silicate liquids: an empirical method of prediction, Am. J. Sci. 272, 870–893, 1972.

[20] M.S. Ghiorso, I.S.E. Carmichael, M.L. Rivers and R.O. Sack, The Gibbs free energy of mixing of natural silicate liquids: an expanded regular solution approximation for the calculation of magmatic intensive variables, Contrib. Mineral. Petrol. 84, 107–145, 1983.

[21] R.A. Lange and I.S.E. Carmichael, Densities of Na_2O-K_2O-CaO-MgOFeO-Fe_2O_3-Al_2O_3-TiO_2-SiO_2 liquids: New measurements and derived partial molar properties, Geochim. Cosmochim. Acta 51, 2931–2946, 1987.

[22] R.S.J. Sparks, The dynamics of bubble formation and growth in magmas: a review and analysis, J. Volcanol. Geotherm. Res. 3, 1–37, 1978.

[23] Y.S. Touloukin, W.R. Judd and R.F. Roy, Physical Properties of Rocks and Minerals, McGraw Hill, New York, 1981.

[24] M.G. Ferrick, A. Qamar and W.F. St. Lawrence, Sources of volcanic tremor, J. Geophys. Res. 87, 8675–8683, 1982.

[25] M. Fehler, Observations of volcanic tremor at Mount St. Helens volcano, J. Geophys. Res. 88, 3476–3484, 1983.

[26] B. Chouet, Resonance of a fluid-driven crack: radiation properties and implications for the source of long-period events and harmonic tremor, J. Geophys. Res. 93, 4375–4400, 1988.

[27] F. Dobran and P. Papale, CONDUIT2: A Computer Program for Modeling Steady-State Two-Phase Flows in Volcanic Conduits, Giardini, Pisa, 1992.

[28] L. Wilson, R.S.J. Sparks and G.P.L. Walker, Explosive volcanic eruptions, IV. The control of magma properties and conduit geometry on eruption column behavior, Geophys. J.R. Astron. Soc. 63, 117–148, 1980.

[29] T.H. Druitt and R.S.J. Sparks, On the formation of calderas during ignimbrite eruptions, Nature 310, 679–681, 1984.

[30] F. Dobran, Global Volcanic Simulation of Vesuvius, Giardini Pisa, 1993.

[31] L. Lirer, T. Pescatore, B. Booth and G.P.L. Walker, Two plinian pumice-fall deposits from Somma–Vesuvius, Italy, Geol. Soc. Am. Bull. 84, 759–772, 1973.

[32] M.F. Sheridan, F. Barberi, M. Rosi and R. Santacroce, A model for Plinian eruptions of Vesuvius, Nature 289, 282–285, 1981.

[33] H. Sigurdsson, S. Carey, W. Cornell and T. Pescatore,

The eruption of Vesuvius in AD 79, Natl. Geogr. Res. 1, 332–387, 1985.

[34] F. Barberi, R. Cioni, R. Santacroce, A. Sbrana and R. Vecci, Variazioni laterali nella distribuzione dei componenti nei depositi delle eruzioni pliniane, Boll. GNV-CRN, Roma, pp. 595–609, 1989.

[35] R. Cioni, P. Marianelli and A. Sbrana, Dynamics of the A.D. 79 eruption: stratigraphic, sedimentological and geochemical data on the successions from the Somma–Vesuvius southern and eastern sectors, Acta Vulcanol. 2, 109–123, 1992.

[36] S. Carey and H. Sigurdsson, Temporal variations in column height and magma discharge rate during the 79 AD eruption of Vesuvius, Geol. Soc. Am. Bull. 99, 303–314, 1987.

[37] F. Barberi and L. Leoni, Metamorphic carbonate ejecta from Vesuvius plinian eruptions. Evidence of the occurrence of shallow magma chambers, Bull. Volcanol. 43, 107–120, 1980.

[38] H. Sigurdsson, W. Cornell and S. Carey, Influence of magma withdrawal on compositional gradients during the AD 79 Vesuvius eruption, Nature 345, 519–521, 1990.

[39] P.C. Hess, Origins of Igneous Rocks, Harvard University Press, Cambridge, 1989.